PHILOSOPHICAL MAGAZINE B, 1981, VOL. 44, NO. 1, 159–174

Effects of transition metal additives on amorphous silicon

By T. SHIMIZU, M. KUMEDA, I. WATANABE and Y. NOUMI
Department of Electronics, Faculty of Technology,
Kanazawa University, Kanazawa 920, Japan

[Received 7 August 1980 and accepted 17 October 1980]

ABSTRACT

Transition metals (Mn, Fe and Ni) have been added to a-Si by a co-sputtering method. The temperature dependence of the electrical conductivity shows that variable-range-hopping-type conduction occurs in these samples. In accordance with this, the magnitude of the thermoelectric power becomes smaller in doped samples. The density of centres due to dangling bonds as determined by E.S.R. decreases when transition elements are added. From these facts, variable-range hopping through the transition element sites is suggested to be the major conduction process in doped samples. The behaviour of the negative magnetoresistance is reasonably explained by this hopping model. A change of the sign of the thermoelectric power from minus to plus by adding transition elements suggests that transition elements are incorporated substitutionally into the amorphous network and act as acceptors. The behaviour of the E.S.R. signals from the transition elements can consistently be explained by such an incorporation scheme. Any shift of the Fermi level toward the valence band must be small because the optical gap changes almost in parallel with twice the high-temperature activation energy for electrical conduction.

§ 1. INTRODUCTION

A large increase in the electrical conductivity has been observed in amorphous silicon (a-Si) by the addition of various kinds of impurities. The mechanism of the increase in hydrogenated a-Si by substitutional doping with shallow impurities (P, B etc.) can easily be understood (Spear 1977). The mechanism of the conductivity increase in non-hydrogenated a-Si caused by the addition of deep impurities such as transition elements (Mn, Fe or Ni), however, is not yet so clear. The investigation of the effect of such deep impurities in a-Si is interesting because a large amount of them can be incorporated into a-Si, in contrast with the case of crystalline Si.

In the present work, sample films have been prepared by co-sputtering Mn, Fe or Ni with Si. Based on the measurements of the electrical conductivity, thermoelectric power, magnetoresistance, optical absorption and E.S.R., a mechanism of the conductivity increase is suggested. Some of the results have previously been reported (Kumeda, Jinno, Watanabe and Shimizu 1977, Shimizu, Kumeda, Watanabe and Kamono 1978, Shimizu, Kumeda, Watanabe and Noumi 1980 c). The present paper describes a full account of these including the results of new experiments.

§ 2. EXPERIMENTAL

Samples were prepared by co-sputtering transition metals, Mn, Fe or Ni with Si using a Varian FP-21 r.f. sputtering system. Since the properties of

0141–8637/81/4401 0159 $02·00

sputtered a-Si depend on the Ar gas pressure during sputtering (Shimizu, Kumeda, Watanabe and Kamono 1979, 1980 a, Shimizu, Kumeda, Watanabe and Kiriyama 1980 b), both a high (150 mTorr) and a low (50 mTorr) Ar gas pressure were used. The ionization gauge for measuring gas pressure is usually calibrated using N_2 gas. The ionization sensitivity of Ar is larger than that of N_2 by about 30%, but this discrepancy was neglected for measuring the Ar gas pressure. Hydrogenated samples were prepared by mixing H_2 into the Ar gas. The H_2 gas pressure quoted in this work is that corrected by considering the ionization sensitivity. The target–substrate spacing was 3·35 cm. Fused quartz was used as a substrate for E.S.R. measurements and glass substrates were used for electrical and optical measurements. The sputtering was performed with 200 W r.f. power (4 W/cm^2) for 1 hour. The film thicknesses ranged from 1·1 to 1·6 μm. The transition element content in several films was measured by electron-probe micro-analysis (EPMA). The results agree within about a factor of two with those estimated from the ratio of the area of the target of the transition metal wafer to that of the Si wafer by taking into account the sputtering rate of each element. Therefore, the content of transition element was determined by the latter method for the results presented in this paper.

Au electrodes were evaporated onto the sample for electrical measurements. The separation between the two Au electrodes was 1 mm for electrical conductivity and magnetoresistance measurements and 10 mm for thermoelectric power measurement. The electrical conductivity was measured at temperatures between 140 and 500 K. Measurements above room temperature were carried out only for samples annealed at 300°C for 2 hours in order to avoid annealing effects during the measurement. The thermoelectric power was measured above room temperature for samples annealed at 300°C for 2 hours. The magnetoresistance was measured at room temperature in a magnetic field up to 14 000 G. The off-balance voltage of a d.c. bridge circuit on applying the magnetic field was used to determine the magnetoresistance. The optical transmittance and reflectance were measured at room temperature and the optical absorption coefficient α was obtained as a function of the photon energy $h\nu$. A plot of $\sqrt{(\alpha h\nu)}$ versus $h\nu$ gives a straight line with a slight upward curvature in the smaller range of α. The extrapolation of the line to $\alpha = 0$ defines the optical gap.

E.S.R. measurements were performed with a JEOL PE 3X spectrometer operating at X-band with a 100 kHz field modulation between liquid nitrogen and room temperature. The centre density associated with the E.S.R. signal was obtained by comparing the absorption area with that of a JEOL standard sample and by assuming spin $S = \frac{1}{2}$. Only in the case of the E.S.R. signal with six hyperfine lines originating from Mn, was S taken as $\frac{5}{2}$.

§ 3. Results

In a-Si films prepared under different sputtering conditions, the electrical conductivity at room temperature σ_{RT} changes by the addition of transition elements as shown in fig. 1. The increase in σ_{RT} is almost independent of the kind of transition element, being as much as a factor of 10^7 at about 5 at.% transition element content. The effect of hydrogenation is not large for

Fig. 1

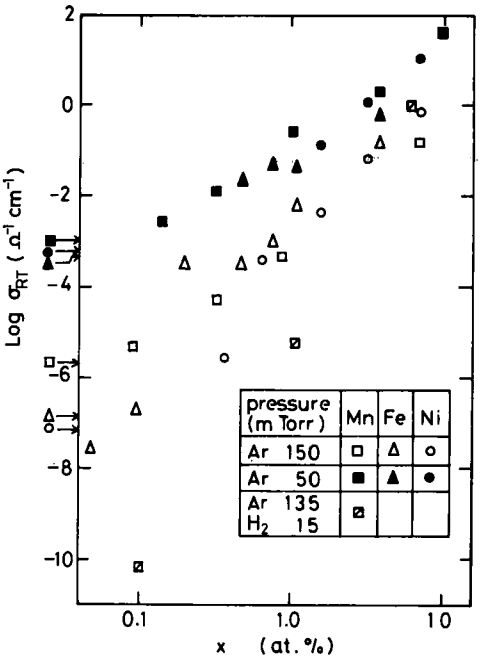

The electrical conductivity at room temperature σ_{RT} as a function of transition element content x in a-S films prepared under different sputtering conditions. Arrows at the ordinate show σ_{RT} for samples without transition elements.

samples doped with transition elements, in contrast with the case of shallow impurities. Although a-Si films without transition element additives show a wide range of values of σ_{RT} ($10^{-3} \sim 10^{-8}$ Ω^{-1} cm^{-1}) depending on the Ar gas pressure during sputtering (Shimizu *et al.* 1979), the range of values becomes narrower when transition elements are added. The temperature dependence of the electrical conductivity σ obeys the variable-range-hopping-type conduction

$$\sigma = \sigma_{0h} \exp\left[-(T_0/T)^{-1/4}\right] \tag{1}$$

below room temperature for as-deposited films both with and without transition elements. The temperature range over which eqn. (1) holds extends toward higher temperatures with the addition of transition elements. The constant T_0 decreases with increasing transition element content, as shown in fig. 2. By annealing at 300°C for 2 hours, an electrical conductivity obeying the activation-type conduction,

$$\sigma = \sigma_0 \exp\left[-E_a/kT\right] \tag{2}$$

appears in a high-temperature range. Figure 3 shows a change of E_a as a function of transition element content. When the temperature range over which the relation of eqn. (2) holds is not wide enough to give a definite value of E_a, a contribution to σ of the variable-range-hopping-type conduction in eqn. (1) is subtracted from the observed value of σ after extrapolating the plot of

log σ versus $T^{-1/4}$ to the higher temperature range. Then, E_a is estimated by assuming σ_0 to be between 10^2 and 10^4 Ω^{-1} cm^{-1}, to which the lower and higher limits of the error bars in fig. 3 correspond respectively. One half of the optical gap, $E_g/2$, is also indicated in fig. 3 for samples prepared both under the high and low Ar gas pressures.

The temperature dependence of the thermoelectric power of a-Si doped with Mn, Fe and Ni are shown in figs. 4, 5 and 6, respectively. Data for undoped a-Si are shown in fig. 5. In contrast with a large negative thermoelectric power for undoped a-Si, doped samples tend to exhibit a small and almost temperature-independent thermoelectric power. The solid curves in figs. 4, 5 and 6 are theoretical ones which will be discussed later.

Figures 7, 8 and 9 show the magnetoresistance $\Delta\rho/\rho$ at room temperature for a-Si doped with Mn, Fe and Ni, respectively, as a function of magnetic field. As is evident from the figures, $\Delta\rho/\rho$ is negative and its absolute value tends to increase with increasing the magnetic field. For samples prepared under the high Ar gas pressure without transition elements, the magnetoresistance could not be measured because of the high resistance of the sample and its temperature fluctuation during the measurement. In the case of the low Ar gas pressure, $|\Delta\rho/\rho|$ becomes larger when small amounts of transition elements are added ($x=0{\cdot}20$ for Fe and $x=0{\cdot}35$ for Ni) than that for $x=0$. In contrast, as the amount of the transition elements increases further, $|\Delta\rho/\rho|$ tends to decrease. In the case of the high Ar gas pressure, such behaviour is not obvious because of the lack of data for the undoped sample, but $|\Delta\rho/\rho|$ decreases at relatively high concentrations of transition elements.

Figure 10 shows the optical gap E_g as a function of transition element content for samples annealed at 300°C for 2 hours. For the sake of comparison, the value of E_g for samples without annealing is shown by the dotted curves. The optical gap, as well as the activation energy for electrical conduction shown in fig. 3, decreases with increasing transition element content.

The density of centres deduced from the E.S.R. signal with $g=2{\cdot}0055$ decreases with increasing transition element content as shown in fig. 11. The g value does not change appreciably, but the linewidth tends to increase when transition elements are added.

Samples doped with Mn prepared under the high Ar gas pressure exhibit, both at room and liquid-nitrogen temperature, an E.S.R. signal which has a hyperfine structure (hfs) with a hfs constant of 93 G (Kumeda *et al.* 1977). At liquid-nitrogen temperature, an E.S.R. signal, which appears to originate from the transition element, is observed for samples doped with Fe or Ni, in addition to the E.S.R. signal due to dangling bonds (Shimizu *et al.* 1980 c). The density of centres associated with these signals is shown in fig. 12 as a function of transition element content. The g values are 2·01–2·04 for Fe and 2·01–2·015 for Ni. The linewidths are 50–90 G for Fe and 30–40 G for Ni. As shown in fig. 12, the densities of centres increase with transition element content up to about 1 at.% and then decrease, but the density associated with the hfs signal from Mn continues to increase with Mn content. The densities for Fe and Ni decrease with rising temperature, while the density associated with the hfs signal from Mn does not depend on temperature. The signals from Fe or Ni do not change appreciably with the Ar gas pressure used during sputtering, but the hfs signal from Mn appears only for Mn-doped samples prepared under

Fig. 2

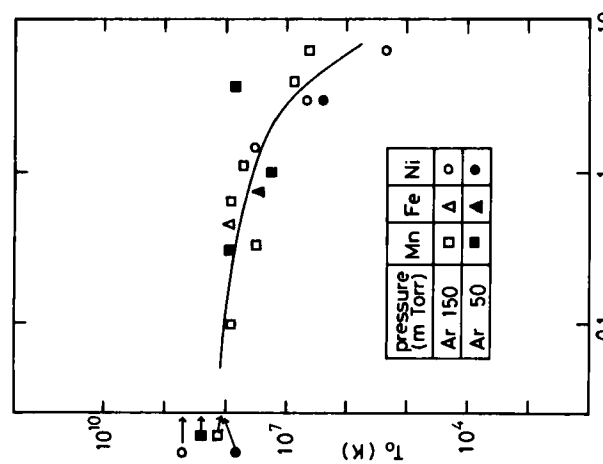

The slope T_0 of log σ versus $T^{-1/4}$ plotted as a function of transition element content x in a-Si films prepared under high and low Ar gas pressures. Arrows at the ordinate show T_0 for samples without transition elements.

Fig. 3

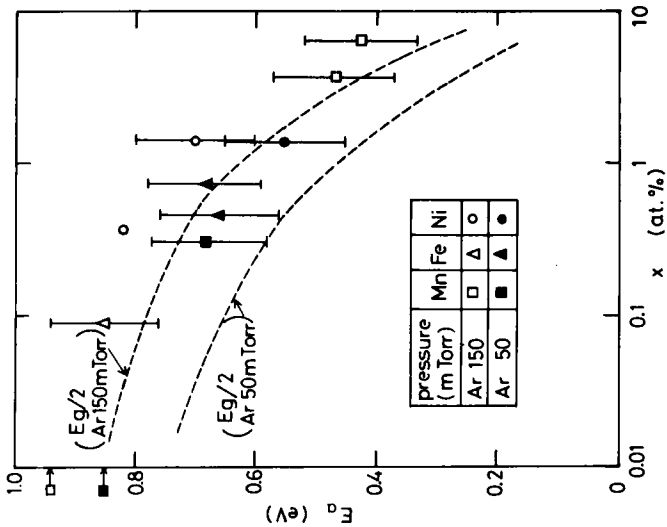

The activation energy E_a for electrical conduction as a function of transition element content x in a-Si films prepared under high and low Ar gas pressures. Samples had been previously annealed at 300°C for 2 hours. For comparison, one half of the optical gap for annealed samples in fig. 10 is shown by dashed curves.

Fig. 4

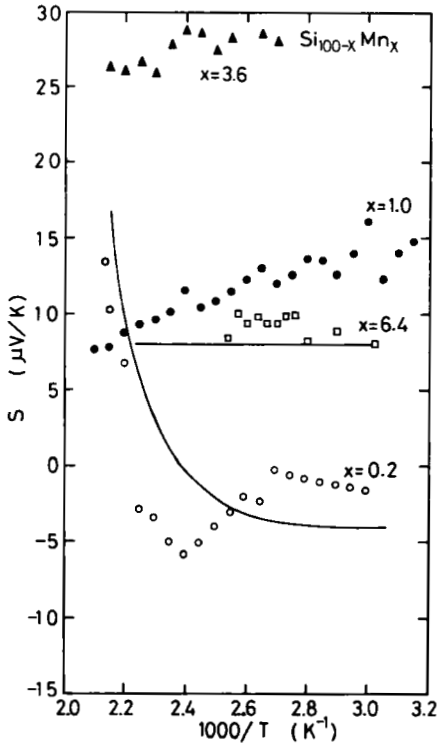

Temperature dependence of the thermoelectric power for a-Si films doped with Mn. Open and closed symbols are for samples prepared under high (150 mTorr) and low (50 mTorr) Ar gas pressures, respectively. Solid curves are theoretical (see the text).

Fig. 5

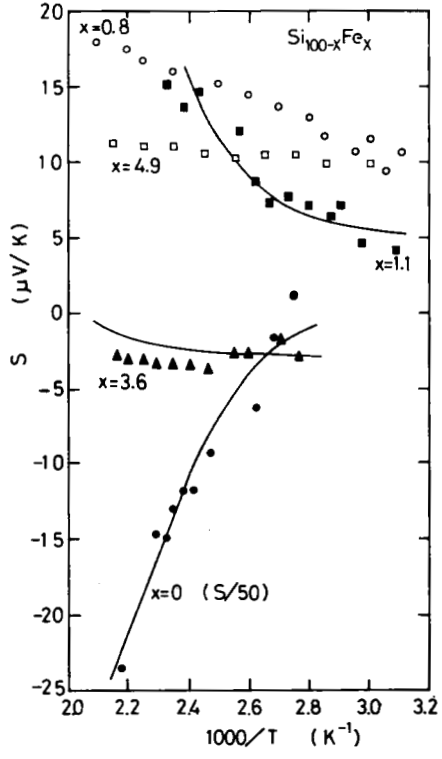

Temperature dependence of the thermoelectric power for a-Si films doped with Fe. Open and closed symbols are for samples prepared under high (150 mTorr) and low (50 mTorr) Ar gas pressures, respectively. Solid curves are theoretical (see the text).

Fig. 6

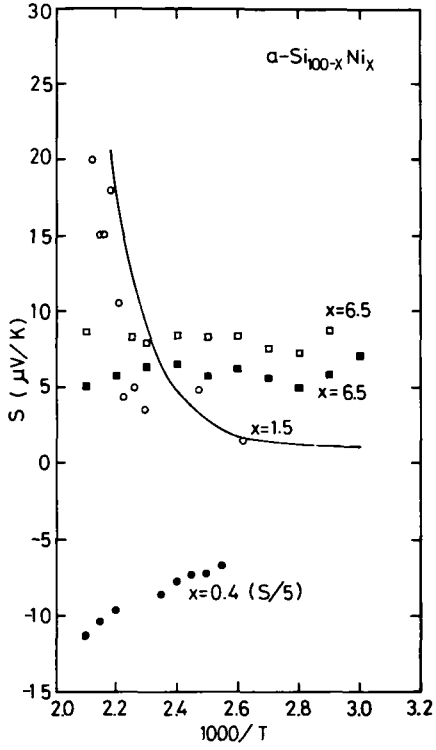

Temperature dependence of the thermoelectric power for a-Si films doped with Ni. Open and closed symbols are for samples prepared under high (150 mTorr) and low (50 mTorr) Ar gas pressures, respectively. Solid curves are theoretical (see the text).

Fig. 7

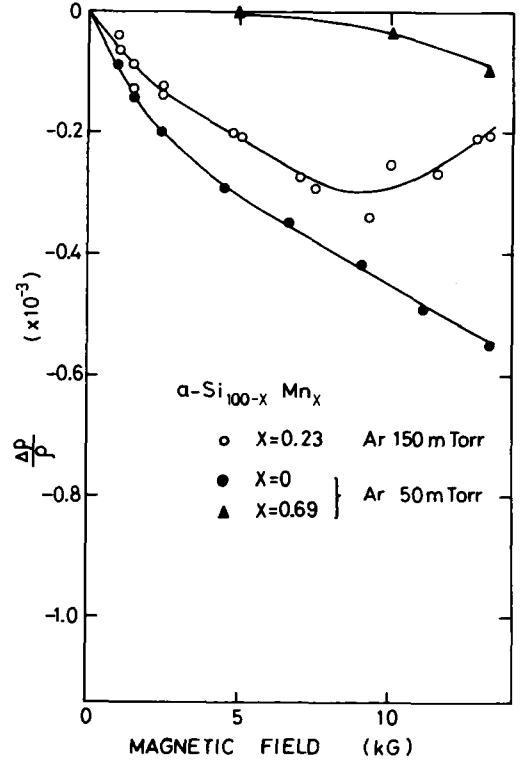

The magnetoresistance as a function of applied magnetic field for a-Si films doped with Mn under high and low Ar gas pressures.

Fig. 8

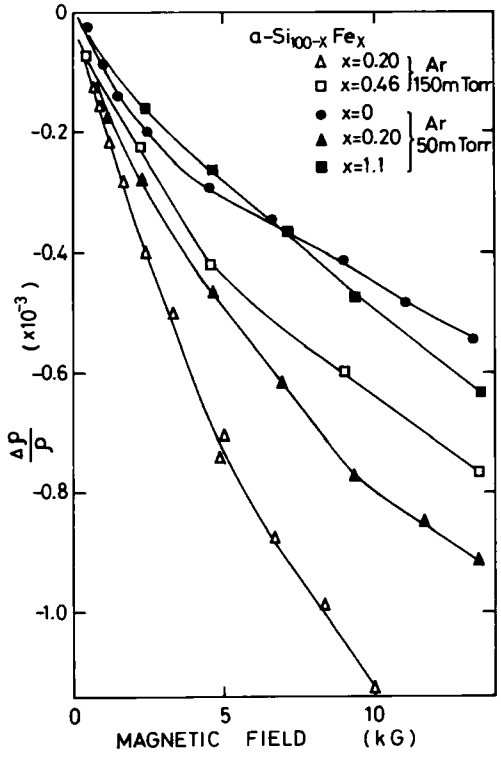

The magnetoresistance as a function of applied magnetic field for a-Si films doped with Fe under high and low Ar gas pressures.

Fig. 9

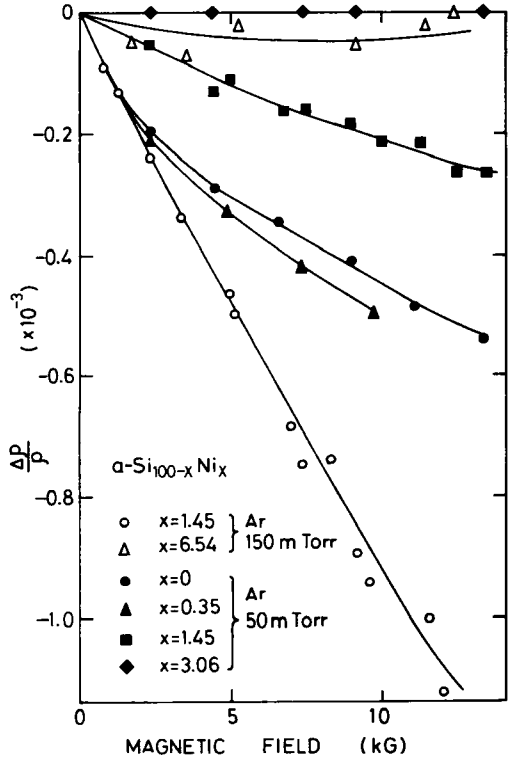

The magnetoresistance as a function of applied magnetic field for a-Si films doped with Ni under high and low Ar gas pressures.

Fig. 10

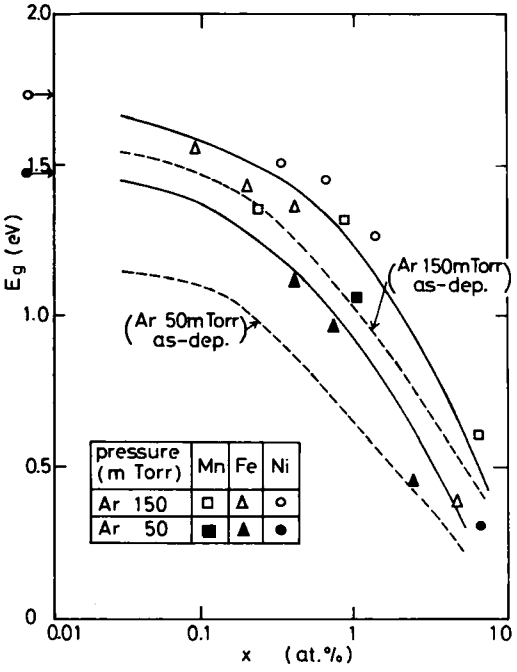

The optical gap E_g as a function of transition element content x for a-Si films prepared under high and low Ar gas pressures. Samples had been previously annealed at 300°C for 2 hours. E_g for samples without annealing is also shown by dashed curves for comparison.

Fig. 11

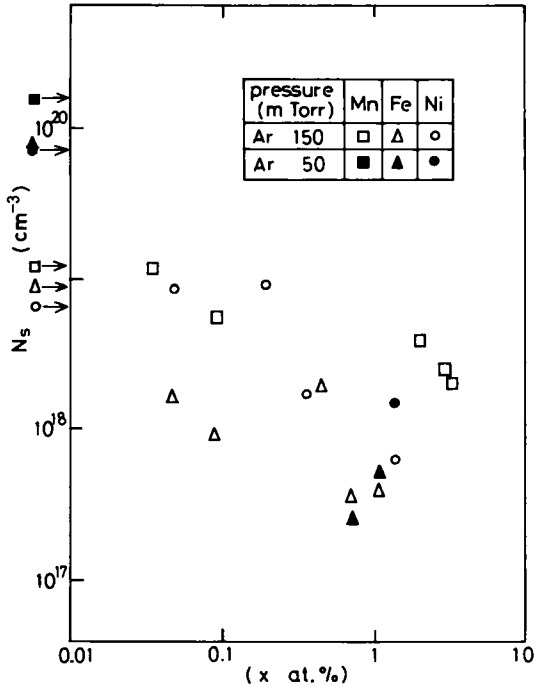

The density of dangling bonds as determined by E.S.R. as a function of transition element content x for a-Si films prepared under high and low Ar gas pressures.

Fig. 12

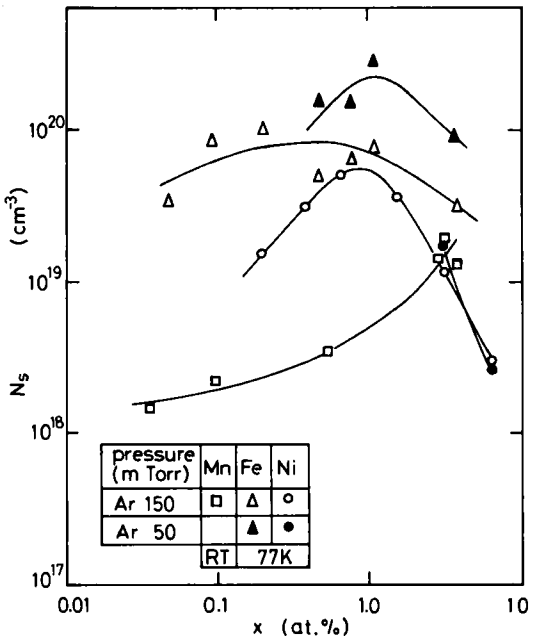

The density of spins due to transition elements as determined by E.S.R. as a function of transition element content x for a-Si films prepared under high and low Ar gas pressures. The density associated with the E.S.R. signal with hfs due to Mn in a-Si films prepared under high Ar gas pressure is different from the previous data (Shimizu *et al.* 1980 c) because of the effect of the overlapping of six hfs lines and also a line from dangling bonds is analysed by computer fitting.

the high Ar gas pressure. Some samples doped with Mn under the low Ar gas pressure exhibit a weak broad E.S.R. signal similar to that observed for Ni-doped samples, but its origin is not clearly distinguishable from some accidental impurities.

§ 4. Discussion

In the last section, we mentioned two series of a-Si films : those prepared under a high Ar gas pressure (150 mTorr) and those prepared under a low Ar gas pressure (50 mTorr). In both series of samples, there are differences in a number of experimental results. a-Si films without transition elements prepared under the high Ar gas pressure have much smaller values of σ_{RT} than those prepared under the low Ar gas pressure, while the former (high-pressure samples) have a lower density of dangling bonds than the latter (low-pressure samples). The smaller σ_{RT} is due to the lower density of dangling bonds through which variable-range hopping takes place. The addition of transition elements, however, gives similar effects for both series of samples despite their intrinsic difference. The density of dangling bonds is reduced by the addition of transition elements, and the differences in σ_{RT} for the two series of samples are reduced. In the following discussion we do not therefore make a distinction

between samples prepared under the two values of Ar gas pressure, concentrating instead on general effects brought about by transition elements in both series of samples.

a-Si films doped with transition elements exhibit the electrical conductivity obeying the variable-range-hopping relation given by eqn. (1). The variable-range-hopping conduction remains dominant up to higher temperatures for samples with transition elements than for samples without them. The appearance of the activation-type conduction at high temperatures suggests that two types of electrical conduction compete.

When two paths of electrical conduction coexist, the thermoelectric power S is given as

$$S = (\sigma_1 S_1 + \sigma_2 S_2)/(\sigma_1 + \sigma_2), \tag{3}$$

where σ_1, S_1 and σ_2, S_2 are the electrical conductivity and thermoelectric power for two different paths. In a-Si, the activation-type conduction and the variable-range-hopping conduction compete (Beyer and Stuke 1974). Therefore, we take σ_1 and σ_2 to be those given by eqns. (2) and (1) respectively. The thermoelectric power associated with the activation-type conduction can be expressed by

$$S_1 = \pm (k/e)[(E_S/kT) + A], \tag{4}$$

where k is the Boltzmann constant, e the elementary charge, E_S an activation energy and A a constant. Plus and minus signs correspond to hole (p-type) and electron (n-type) conduction. The thermoelectric power associated with variable-range-hopping conduction has been calculated (Böttger and Bryksin 1976), but no conclusive result has been obtained. Experiments show that its magnitude is small and only slightly temperature-dependent (Beyer and Stuke 1974). If we assume it to be constant, the thermoelectric power given by eqn. (3) will have a temperature dependence as shown schematically in fig. 13. The contribution from the activation-type conduction is dominant at higher temperatures and that from the variable-range hopping is dominant at lower temperatures. The behaviour of the experimental results can be understood by the two-path model described here. By comparing fig. 13 with figs. 4, 5 and 6, it is found that an n-type activation-type contribution appearing in undoped a-Si changes to a p-type activation-type contribution by the addition of relatively small amounts of transition elements. For samples with higher transition element content, the thermoelectric power is small and almost temperature-independent, indicating that the variable-range hopping becomes dominant up to higher temperatures. The result is consistent with the observed temperature dependence of the electrical conductivity in which the temperature range over which the variable-range hopping is dominant extends to higher temperatures by the addition of transition elements. The solid curves in figs. 4, 5 and 6 are drawn by choosing parameters which are shown in the table. It should be noted that these parameters are not inconsistent with those obtained from the electrical conductivity measurements.

According to a theory of the magnetoresistance in the hopping regime proposed by Osaka (1979), a negative magnetoresistance is expected whose absolute value increases with increasing applied magnetic field when the positive

Fig. 13

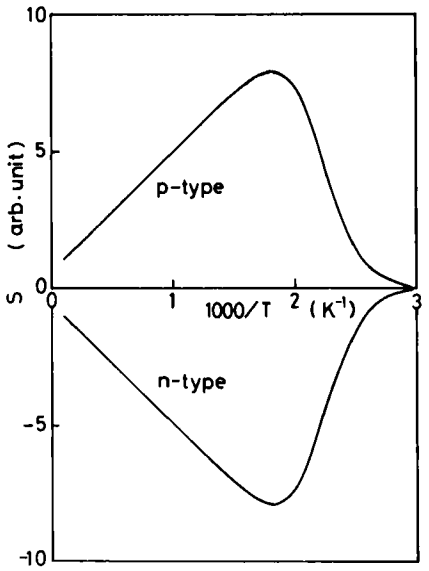

Schematic diagram of temperature dependence of the thermoelectric power when activation-type conduction and variable-range-hopping conduction are competing.

Parameters chosen for the calculation of eqn. (3) with eqns. (1), (2) and (4). The value of A in eqn. (4) is assumed to be 1·16. The sign of eqn. (4) is negative only for the undoped sample, being positive for all other doped samples.

Impurity	Undoped	Mn		Fe		Ni
Ar pressure	Low	High	High	Low	Low	High
x (at.%)	0	0·2	6·4	1·1	3·6	1·5
σ_0 (Ω^{-1} cm^{-1})	10^4	10^4	10^3	10^4	10^3	10^4
E_a (eV)	0·8	0·8	0·52	0·62	0·6	0·8
E_S (eV)	0·8	0·8	0·52	0·62	0·6	0·6
σ_{0h} (Ω^{-1} cm^{-1})	2×10^6	$5{\cdot}4\times10^4$	$7{\cdot}1\times10^2$	10^6	$4{\cdot}4\times10^4$	$1{\cdot}2\times10^2$
T_0 (K)	2×10^8	4×10^7	2×10^6	$3{\cdot}4\times10^7$	10^7	$8{\cdot}2\times10^6$
S_2 (μV/K)	0	−4	+8	+5	−3	+1

component of the magnetoresistance is negligible because of a small local magnetic field. The theory further predicts that the magnitude of the negative component of the magnetorsistance increases with an increase of the constant T_0 in eqn. (1), the electron correlation energy and the shift of the g value from the free-electron value of 2·0023. When transition elements are added to a-Si, variable-range hopping through transition element sites becomes the dominant transport path instead of the variable-range hopping through dangling-bond sites, as will be discussed later. The wavefunction of an electron in 3d orbitals of the transition elements is considered to be more localized than

that of the dangling bonds. This consideration is supported by the fact that the decay length of the localized wavefunction has been estimated to be 5 Å (Shimizu *et al.* 1980 b) or 4·7 Å (Kumeda and Shimizu 1980) for dangling bonds and 2 Å (Shimizu *et al.* 1978) for Mn, from the slope of a linear relation between $\log \sigma_{RT}$ versus $N^{-1/4}$, where N is the density of the hopping centres (Stuke 1976). Hence, the electron correlation energy should be larger for transition elements than for dangling bonds, and so the magnitude of the negative component of the magnetoresistance increases by the addition of small amounts of transition elements. Values of g for transition elements ($g = 2{\cdot}01$–$2{\cdot}04$) are larger than that for dangling bonds ($g = 2{\cdot}0055$), which may also increase the magnitude of the negative component of the magnetoresistance. Thus the increase in the absolute value of the negative magnetoresistance for samples doped with small amounts of transition elements in the case of low Ar gas pressure ($x = 0{\cdot}20$ for Fe and $x = 0{\cdot}35$ for Ni) may be explained by these two reasons.

On the other hand, the decrease of the absolute value of the negative magnetoresistance for samples doped more heavily with transition elements ($x > 1{\cdot}0$) is considered to be consistent with the decrease of T_0 in fig. 2.

The magnitude of the optical gap and that of twice the activation energy for electrical conduction are fairly close, and they decrease in a parallel manner with increasing transition element content, as seen from fig. 3. Hence, the addition of transition elements does not give rise to a large shift of the Fermi level, in contrast with shallow impurities which move the Fermi level towards the valence or conduction band (Spear 1977). However, a small shift of the Fermi level should take place towards the valence band by the addition of transition elements because the thermoelectric power shows p-type conduction for samples doped with transition elements, as mentioned above. The amount of the shift is estimated to be less than 0·1 eV.

Kishimoto and Morigaki (1979) have reported on properties of a-Si films doped with another deep impurity, Au. The Au atoms bring about a shift of the Fermi level toward the valence band, as do transition elements. However, in the case of the addition of Au atoms, a rather large change of the activation energy in the thermoelectric power occurs by the addition of 0·4 at.% of Au atoms, in contrast with a small change of the optical gap, and the magnitude of the activation energy for electrical conduction is far smaller than the magnitude of one-half of the optical gap. Therefore, the shift in the Fermi level is larger in the case of Au addition than it is for the transition elements. This fact suggests that Au atoms form a shallower acceptor level than do transition elements.

The increase of the temperature range over which eqn. (1) holds, as well as the decrease in the magnitude of the thermoelectric power and the decrease in the absolute value of the negative magnetoresistance, confirm that variable-range-hopping conduction is dominant in samples doped with transition elements. The decrease in T_0 in eqn. (1) with increase of transition element content indicates the increase in the density of states at the Fermi level $N(E_F)$, because T_0 is given by (Ambegaokar, Halperin and Langer 1971)

$$T_0 = 16/[ka^3 N(E_F)], \tag{5}$$

where a is the decay length of the localized wavefunction. The density of dangling bonds as determined by E.S.R., however, decreases with increasing

transition element content, as shown in fig. 9. Therefore, variable-range hopping through transition element sites is considered to be the main conduction mechanism.

A noticeable result is that three of the transition elements, Mn, Fe and Ni, have a similar effect on σ_{RT}, implying that the decay lengths a of the wave-function, for these elements are almost the same, since the hopping rate is highly sensitive to a (see eqn. (5)).

It is not clear at present how the transition elements are incorporated into the a-Si network, but some speculations can be made. The acceptor character of the transition elements suggests that they are substitutionally incorporated and are in negative charge states. No structural investigation has been reported for transition elements in a-Si, but both EXAFS (Oyanagi, Tsuji, Hosoya, Minomura and Fukamachi 1980) and neutron diffraction (Yamada, Endoh, Ishikawa and Watanabe 1980) experiments suggest that Ni is incorporated substitutionally in a-Ge. In crystalline Si, the energy of the 3d orbitals of transition elements incorporated substitutionally is split into a triplet and a doublet, the latter having a lower energy (Ludwig and Woodbury 1962). If we assume that Fe and Ni are in negative single charge states, the electronic configurations $3d^5$ and $3d^7$ are expected for substitutionally incorporated, fourfold-coordinated Fe and Ni atoms respectively, and, as can be seen from Fig. 14, the orbital angular momentum in both cases becomes zero, which is necessary for the E.S.R. signal to be detectable. If this assumption is correct, Fe and Ni have spins $S=\frac{5}{2}$ and $\frac{3}{2}$, so that the centre densities for Fe and Ni estimated by assuming $S=\frac{1}{2}$ shown in fig. 12 should be reduced by factors of $\frac{3}{35}$ and $\frac{1}{5}$, respectively. The decrease in the centre density due to transition element contents of over 1 at.% may be explained by assuming that the Fermi level shift makes the electronic configuration of the transition elements change to configurations $Fe^0(3d^4)$ and $Ni^0(3d^6)$ which have non-zero orbital angular momentum, as seen from fig. 14. The decrease in the centre density with rising temperature is also explained by the thermal excitation of transition atoms to the electronic configuration not exhibiting E.S.R. (Shimizu *et al.* 1980 c). A singly charged Mn^- centre in a substitutional site, however, has an electronic configuration of $3d^4$ which does not quench the orbital angular momentum as seen fig. 14, and this produces no E.S.R. signal. This may be the reason why samples doped with Mn under the low Ar gas pressure barely exhibit the E.S.R. signal.

Fig. 14

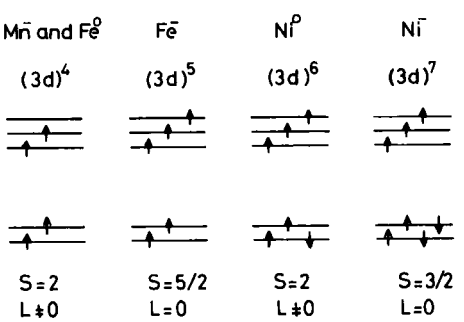

Electronic configuration of transition elements substitutionally incorporated in Si.

Some small fraction of transition elements in samples prepared under the high Ar gas pressure can reside rather freely in voids, because a-Si prepared under the high Ar gas pressure is found to have a porous structure (Shimizu *et al.* 1980 b). $Mn^{2+}(3d^5)$ in such loosely bound sites can explain the observed large hfs constant, close to that for free Mn^{2+} ions, for samples doped with Mn under the high Ar gas pressure. However, $Fe^{2+}(3d^6)$ or $Ni^{2+}(3d^8)$ in voids will have a non-zero orbital angular momentum so that no E.S.R. signal is expected.

§ 5. Conclusions

Transition metals (Mn, Fe or Ni) have been added to a-Si by a co-sputtering method. From measurements of the electrical conductivity, thermoelectric power, magnetoresistance, optical gap and E.S.R., the following conclusions are obtained.

(1) The electrical conductivity increases considerably by the addition of transition elements. The increase is almost independent of the kind of transition element and reaches 7 orders of magnitude at a transition element content of about 5 at.%.

(2) The increase of the electrical conductivity results mainly from the generation of electron hopping states due to transition elements below and near the intrinsic Fermi level, and thereby from variable-range hopping through the transition element sites. The conductivity is almost independent of the kind of element, implying that the decay lengths of the electron wavefunctions for these elements are very similar.

(3) The addition of a small amount of these elements causes an increase in the negative magnetoresistance, and further addition tends to reduce it. These results can be explained by variable-range hopping through the transition element sites.

(4) These transition elements cause the Fermi level to shift slightly towards the valence band, making the thermoelectric power change to a positive value. Therefore they are supposed to be incorporated at substitutional positions in the a-Si network and to be in negative charge states. Such an incorporation scheme can explain the behaviour of the E.S.R. associated with the transition elements.

Acknowledgments

The authors wish to thank Mr. M. Asamura and Mr. N. Yamamoto for their technical assistance. The authors also wish to thank Dr. M. Suhara for the use of the E.S.R. spectrometer at the Faculty of Science of Kanazawa University. Helpful advice from Dr. S. Tsugane and Professor K. Morigaki on measuring magnetoresistance is appreciated. This work is partly supported by a Grant-in-Aid for Scientific Research (No. 446051) from the Ministry of Education, Science and Culture in Japan.

References

Ambegaokar, V., Halperin, B. I., and Langer, J. S., 1971, *Phys. Rev.* B, **4**, 2612.

Beyer, W., and Stuke, J., 1974, *Amorphous and Liquid Semiconductors*, edited by J. Stuke and S. Brenig (London : Taylor & Francis Ltd), p. 251.

BÖTTGER, H., and BRYKSIN, V. V., 1976, *Phys. Stat. Sol.* (b), **78**, 415.
KISHIMOTO, N., and MORIGAKI, K., 1979 a, *J. phys. Soc. Japan*, **46**, 497 ; 1979 b, *Ibid.*, **46**, 846.
KUMEDA, M., JINNO, Y., WATANABE, I., and SHIMIZU, T., 1977, *Solid St. Commun.*, **23**, 933.
KUMEDA, M., and SHIMIZU, T., 1980, *Jap. J. appl. Phys.*, **19**, L197.
LUDWIG, G. W., and WOODBURY, H. H., 1962, *Solid State Physics*, Vol. 13 (New York, London : Academic Press), p. 263.
OSAKA, Y., 1979, *J. phys. Soc. Japan*, **47**, 729.
OYANAGI, H., TSUJI, K., HOSOYA, S., MINOMURA, S., and FUKAMACHI, T., 1980, *J. non-crystalline Solids*, **35–36**, 555.
SHIMIZU, T., KUMEDA, H., WATANABE, I., and KAMONO, K., 1978, *Solid St. Commun.*, **26**, 445 ; 1979, *Jap. J. appl. Phys.*, **18**, 1923 ; 1980 a, *J. non-crystalline solids*, **35–36**, 303.
SHIMIZU, T., KUMEDA, M., WATANABE, I., and KIRIYAMA, Y., 1980 b, *Jap. J. appl. Phys.*, **19**, L235.
SHIMIZU, T., KUMEDA, M., WATANABE, I., and NOUMI, Y., 1980 c, *J. non-crystalline Solids*, **35–36**, 645.
SPEAR, W. E., 1977, *Adv. Phys.*, **26**, 811.
STUKE, J., 1976, *Proceedings of the Sixth International Conference on Amorphous and Liquid Semiconductors*, edited by B. T. Kolomiets (Leningrad : Nauka), p. 193.
YAMADA, K., ENDOH, U., ISHIKAWA, U., and WATANABE, N., 1980, *J. phys. Soc. Japan*, **48**, 922.